Determination of the reaction plane in ultrarelativistic nuclear collisions

Jean-Yves Ollitrault*
Service de Physique Théorique, CE-Saclay, F-91191 Gif-sur-Yvette Cedex, France
(Received 18 March 1993)

If the particles produced in a nuclear collision undergo collective flow, the reaction plane can in principle be determined through a global event analysis. We show here that collective flow can be identified by evaluating the reaction plane independently in two separate rapidity intervals, and studying the correlation between the two results. We give an analytical expression for the correlation function between the two planes as a function of their relative angle. We also discuss how this correlation function is related to the anisotropy of the transverse momentum distribution.

PACS number(s): 25.75.+r, 12.38.Mh, 24.60.Ky, 47.75.+f

I. INTRODUCTION

In searching for evidence of the formation of a quark-gluon plasma in ultrarelativistic nucleus-nucleus collisions, one is led to address the question of whether the matter produced in these collisions can be considered, at least locally, to be in thermal equilibrium. Local equilibrium implies that the matter behaves collectively, which may have observable consequences. When collective flow is present, the evolution of the system is determined by the pressure gradient, and is therefore strongly influenced by geometrical factors (nuclear size, impact parameter, . . .). Effects of geometry on global event shapes have made possible the detection and the study of the collective flow of nuclear matter at colliding energies up to 1 GeV per nucleon [1]. However, few such studies have been undertaken at ultrarelativistic energies, and no conclusion has been drawn so far [2].

Most analyses at intermediate energies have been concerned with the determination of the flow direction, which is the direction of maximum kinetic-energy flow. However, the flow angle (angle between collision axis and flow direction) decreases with increasing energy and cannot be measured at ultrarelativistic energies; this is because longitudinal momenta are much larger than transverse momenta. When it can be measured, the flow direction gives an experimental determination of the reaction plane, which is the plane spanned by the collision axis and the impact parameter. The latter can also be determined independently by measuring the transverse momentum transfer between target and projectile regions [3]. Although this method has not been successful at the CERN Super Proton Synchrotron SPS [2], it has been recently argued that it should give results with heavy nuclei [4].

Since the flow direction merges with the collision axis at ultrarelativistic energies, whether or not there is collective behavior, evidence for collective flow should be sought for rather in the transverse directions. Note further that while analyses carried out at intermediate energies are mostly concerned with nucleons, the large number of mesons created at ultrarelativistic energies in the central rapidity region offers an opportunity to study collective flow, not only of spectators and/or participant nucleons, but also among the produced particles. Starting from these observations, we have proposed a new signature in a previous work [5]. The idea is that for peripheral collisions, the region where nucleon-nucleon collisions take place, when projected onto the transverse plane, is anisotropic: it has a smaller size in the direction of the impact parameter than in the perpendicular direction. This causes the matter produced in the central rapidity region to flow preferentially in the direction of the impact parameter, which results in a corresponding anisotropy of the transverse momentum distribution. This anisotropy should increase with the impact parameter.

We propose to study collective flow in the plane orthogonal to the principal flow direction (here, the collision axis). This has also been done at lower energies [6], where it was found that matter escapes preferentially in the direction orthogonal to the reaction plane. This was referred to as the *squeeze-out* effect. By contrast, we predict a larger flow *in* the reaction plane. However, this is only an apparent contradiction since the effects that come into play are very different [7]. Squeeze-out results from an interaction between the participant nucleons, which try to escape the fireball, and the spectators which block their path in the reaction plane. But at ultrarelativistic energies, the time it takes for the nuclei to cross each other is so short that the particles produced in the central rapidity region do not "see" the spectators. Anisotropy results from the interaction of particles in the central rapidity region among themselves.

The main problem one usually encounters in global analyses is that fluctuations occur due to the finite multiplicity, which may hide collective effects [8]. In this article we would like to show how statistical and dynamical effects can be separated in the anisotropy analysis. The idea is that in a given event, one can perform two measurements of the reaction plane by doing global analysis with two separate subsets of the emitted particles (by

*Electronic address: ollie@amoco.saclay.cea.fr

selecting, for instance, the particles produced in two separate rapidity intervals). Then the difference between the two results gives a direct measure of the dispersion due to statistical fluctuations.

In Sec. II we recall the definitions of the variables we use in the global analysis [5]. In Sec. III we give a general discussion of finite multiplicity fluctuations. The main results are contained in Sec. IV where we calculate, under quite general assumptions, the correlation function between the two measurements of the reaction plane. We show how to measure the ratio of dynamical to statistical effects directly from the experiment. In Sec. V we show how this can be used to isolate the dynamical part in the anisotropy. The relevance of this work to current and future experiments is discussed in Sec. VI.

II. GLOBAL ANALYSIS

In flow analyses, an event is characterized by means of global observables describing its shape. At ultrarelativistic energies, we are only interested in the transverse directions. We therefore define the 2×2 transverse sphericity [9] tensor $S^{\perp}$ by

$$S_{ij}^{\perp}=\sum_{\nu=1}^{M} w(\nu)u_i(\nu)u_j(\nu) , \tag{1}$$

where $(u_1(\nu),u_2(\nu))$ is the unit vector parallel to the transverse momentum of the νth particle, $w(\nu)$ is a weight, and the sum runs over all the particles detected in a given rapidity interval. If there is no particle identification, $w(\nu)$ can be chosen to be equal to some function of the transverse energy $E_T(\nu)$ deposited by the particle in the calorimeter; for instance, $w(\nu)=E_T^{\beta}(\nu)$, with β equal to some real constant. Collective flow usually results not only in a larger number of particles emitted in the flow direction, but also in a higher energy per particle in this direction, so that β should be taken positive; for instance, $\beta=1$. Which is the best weight to consider should be determined on the basis of a more careful analysis. However, the results which are presented here do not depend on such details.

$S_{ij}^{\perp}$ has three independent components and is therefore fully determined by its two eigenvalues f_1 and f_2 (we choose $f_1\geq f_2$) and the angle θ between the x axis and the eigenvector associated with f_1, with $-\pi/2\leq\theta\leq\pi/2$. Instead of f_1 and f_2 we choose the variables $\mathcal{E}$ and α defined by

$$\begin{aligned}\mathcal{E}&=\mathrm{tr}S^{\perp}=f_1+f_2 ,\\ \alpha&=\frac{f_1-f_2}{f_1+f_2} .\end{aligned} \tag{2}$$

$S^{\perp}$ can then be expressed as a function of $\mathcal{E}$, α, and θ:

$$S^{\perp}=\frac{\mathcal{E}}{2}\begin{pmatrix}1+\alpha\cos2\theta & \alpha\sin2\theta\\ \alpha\sin2\theta & 1-\alpha\cos2\theta\end{pmatrix} . \tag{3}$$

α measures the relative difference between the eigenvalues of $S^{\perp}$, i.e., the anisotropy of the momentum distribution. As we said in Sec. I, collective flow results in anisotropy for peripheral collisions [5]. Hydrodynamical calculations predict that α decreases linearly with the multiplicity or the transverse energy (which are measures of the impact parameter). The highest value of α, obtained for very peripheral collisions, is about 0.25–0.3 for a Pb-Pb collision, and slightly less, about 0.2, for a S-W collision.

There is a larger flow in the direction of the impact parameter than in the direction perpendicular to the reaction plane [6]. Thus we expect that the principal axis associated with the larger eigenvalue f_1 is the direction of the impact parameter. Since $S^{\perp}$ is directly measurable, this in turn gives an experimental measurement of the orientation of the reaction plane. However, this estimate is reliable only if the measured anisotropy originates from collective flow. Statistical fluctuations related to the finite multiplicity also generate anisotropy, which must be disentangled from the dynamical anisotropy created by collective behavior. It is the purpose of this paper to show how this can be done experimentally.

III. FINITE MULTIPLICITY FLUCTUATIONS

Macroscopically, a collision between two spherical nuclei is fully characterized by the colliding energy and the impact parameter. However, particle emission is the result of microscopic processes (parton-parton or nucleon-nucleon collisions) which are not described by these macroscopic variables. For fixed energy and impact parameter, this results in statistical fluctuations of global macroscopic quantities such as the sphericity tensor $S_{ij}^{\perp}$. Now, since particles are created independently at different points in the system, it is reasonable to assume that $S_{ij}^{\perp}$ is the sum of a large number of independent random contributions. Then the central limit theorem states that the probability law of $S_{ij}^{\perp}$ is Gaussian. To avoid having to deal with too many indices, we rearrange the three independent components of $S_{ij}^{\perp}$ into a three-vector S whose components S_i are defined as

$$\begin{aligned}S_1&=S_{11}^{\perp}+S_{22}^{\perp}=\mathcal{E} ,\\ S_2&=S_{11}^{\perp}-S_{22}^{\perp}=\mathcal{E}\alpha\cos2\theta ,\\ S_3&=2S_{12}^{\perp}=\mathcal{E}\alpha\sin2\theta .\end{aligned} \tag{4}$$

The most general Gaussian probability distribution for S_i is of the form

$$\frac{dP}{dS_1dS_2dS_3}\propto\exp[-({}^tS-{}^t\bar{S})T^{-1}(S-\bar{S})/2] , \tag{5}$$

where $\bar{S}=\langle S\rangle$ is the average value of S and T is the 3×3 covariance matrix defined by

$$T_{ij}=\langle S_iS_j\rangle-\bar{S}_i\bar{S}_j . \tag{6}$$

If one considers two independent random variables S and S' with Gaussian probabilities such as (5), with respective covariance matrices T and T', the probability of $S+S'$ is Gaussian, with a covariance matrix equal to $T+T'$. Thus T_{ij} is proportional to the number of particles M used in the analysis.

Since the system is symmetric with respect to the reaction plane for spherical nuclei, so must be the probability

(5). We choose x to be the direction of the impact parameter. Then the symmetry with respect to the reaction plane changes θ into $-\theta$. Equation (5) is invariant under this transformation if

$$\bar{S}_3=0 , \quad T_{13}=T_{23}=0 . \tag{7}$$

Thus $\bar{S}$ depends only on two parameters:

$$\bar{S}_1=\bar{\mathcal{E}} , \quad \bar{S}_2=\bar{\mathcal{E}}\bar{\alpha} . \tag{8}$$

$\bar{\alpha}$ represent the anisotropy associated with $\bar{S}$, that is, the anisotropy in the emission law. Although $\bar{S}$ is the average value of S, $\bar{\alpha}$ is in general not equal to the average value of α, $\langle\alpha\rangle$: for an isotropic emission, $\bar{\alpha}=0$, but in general $\alpha>0$ with a finite number of particles. While $\bar{\alpha}$ represents the anisotropy associated with macroscopic effects—for instance, with collective flow—the average value $\langle\alpha\rangle$ also receives a contribution from finite multiplicity fluctuations.

If the emission is weakly anisotropic, i.e., if $\bar{\alpha}\ll 1$, the covariance matrix T is approximately the same as for an isotropic distribution. For an isotropic distribution, the probability (5) must be invariant under rotations, that is, under transformations $\theta\rightarrow\theta+\theta_0$ with θ_0 fixed. This implies

$$T_{12}=0 , \quad T_{22}=T_{33} . \tag{9}$$

Then the probability (5) can be integrated over $\mathcal{E}$ with the result [5]

$$\frac{dP}{d\alpha\, d\theta}=\frac{4\alpha}{\pi\sigma^2}\exp\left[-\frac{\bar{\alpha}^2+\alpha^2-2\alpha\bar{\alpha}\cos 2\theta}{\sigma^2}\right] \tag{10}$$

with

$$\sigma=\sqrt{2T_{22}}/\bar{\mathcal{E}} . \tag{11}$$

σ is the order of magnitude of the anisotropy created by statistical fluctuations alone, as can be seen easily if $\bar{\alpha}=0$: the probability distribution for α, apart from the pre-exponential factor α which arises from the Jacobian transforming $(\alpha,\mathcal{E},\theta)$ into (S_1,S_2,S_3), is a Gaussian of width $\sigma/\sqrt{2}$. Note that since both T_{22} and $\bar{\mathcal{E}}$ are proportional to the number of particles M used in the analysis, σ scales like $1/\sqrt{M}$. For an uncorrelated emission of identical particles, one finds $\sigma=(1/\sqrt{M})\sqrt{\langle w^2\rangle}/\langle w\rangle$ where w is the weight of the particle in the sphericity tensor, Eq. (1). We have chosen to normalize Eq. (10) to unity in the interval $[0,\pi/2]$ (rather than $[-\pi/2,\pi/2]$ because the function is even), that is,

$$\int_0^{\pi/2}d\theta\int_0^1 d\alpha\frac{dP}{d\alpha\, d\theta}=1 .$$

This will be checked below.

It is convenient to express the probability as a function of the scaled quantities

$$\chi=\alpha/\sigma \quad \text{and} \quad \bar{\chi}=\bar{\alpha}/\sigma . \tag{12}$$

Equation (10) becomes then

$$\frac{dP}{d\chi\, d\theta}=\frac{4\chi}{\pi}\exp(-\bar{\chi}^2-\chi^2+2\bar{\chi}\chi\cos 2\theta) . \tag{13}$$

This equation only involves the dimensionless parameter $\bar{\chi}$, which will play a crucial role in our analysis. Physically, $\bar{\chi}$ represents the ratio of the anisotropy $\bar{\alpha}$ generated by dynamical collective effects to the typical anisotropy σ yielded by statistical fluctuations. Note that strictly speaking, Eq. (13) also involves the parameter σ since χ varies from 0 to $1/\sigma$. However, $\sigma\ll 1$ for a large system and the probability (13) decreases exponentially for $\chi\gg 1$. Thus we will let χ vary from 0 to $+\infty$ when we integrate over χ.

Equation (13) can be integrated over θ using the modified Bessel function I_0 defined in Eq. (A2). One gets then the distribution of the scaled anisotropy χ:

$$\frac{dP}{d\chi}=2\chi\exp(-\bar{\chi}^2-\chi^2)I_0(2\bar{\chi}\chi) . \tag{14}$$

To check that this distribution is normalized to unity, we integrate (14) by parts and use the relation $I_1(z)=dI_0/dz$. Then the formula

$$\int_0^{+\infty}\exp(-\chi^2)I_\nu(2\bar{\chi}\chi)d\chi=\frac{\sqrt{\pi}}{2}\exp\left[\frac{\bar{\chi}^2}{2}\right]I_{\nu/2}\left[\frac{\bar{\chi}^2}{2}\right] \tag{15}$$

with $\nu=1$ gives the result, using the fact that

$$I_{1/2}(z)=2\sinh z/\sqrt{2\pi z} .$$

In principle, the distribution (14) can be compared to the experimental distribution of the anisotropy α: $\bar{\chi}$ and the scale factor σ can be fitted so as to obtain the best agreement with the data. However, this may be difficult in practice, as we are going to see shortly. Figure 1

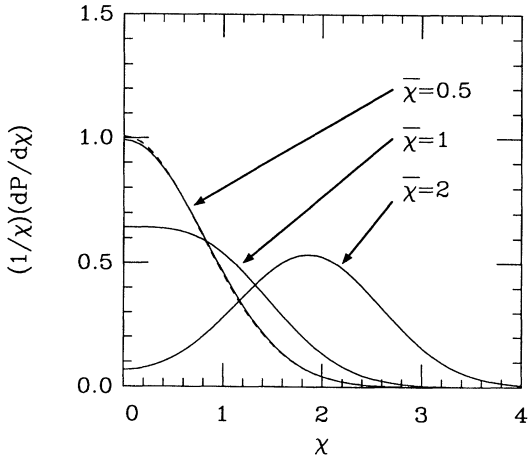

FIG. 1. The solid lines display the values of $(1/\chi)(dP/d\chi)$, given by Eq. (14), as a function of χ for three values of the parameter $\bar{\chi}$. The dashed line is an approximation to the curve $\bar{\chi}=0.5$ by a Gaussian corresponding to the same average value $\langle\chi\rangle$ of χ, calculated from Eq. (26) (see Sec. V). All curves are normalized to unity: $\int_0^{+\infty}(1/\chi)(dP/d\chi)d\chi=1$.

displays $(1/\chi)(dP/d\chi)$ [that is, the distribution (14) divided by the factor χ arising from the Jacobian] for three values of the parameter $\bar{\chi}$. For $\bar{\chi}=0$ (no collective flow), this quantity would be a Gaussian of width $1/\sqrt{2}$ centered at $\chi=0$ as can be seen from Eq. (14). On the other hand, if $\bar{\chi}>1$, one easily shows that $(1/\chi)(dP/d\chi)$ reaches its maximum at a nonvanishing value of χ, which becomes closer to $\bar{\chi}$ as $\bar{\chi}$ increases. This can be used [5] as a signature of collective flow. If $\bar{\chi}<1$, however, the maximum is reached at $\chi=0$ and the distribution is very close to a Gaussian as illustrated in Fig. 1 for $\bar{\chi}=0.5$. Thus, the effect of $\bar{\chi}$ is simply to increase the width of the χ distribution, compared to $\bar{\chi}=0$. Since the α distribution has the same shape as for $\bar{\chi}=0$ it is impossible to extract $\bar{\chi}$ from the anisotropy distribution alone.

Equation (13) can also be integrated over χ, which yields the probability distribution of the angle θ:

$$\frac{dP}{d\theta}=\frac{2}{\pi}\exp(-\bar{\chi}^2)\{1+\sqrt{\pi}\bar{\chi}\cos2\theta[1+\mathrm{erf}(\bar{\chi}\cos2\theta)]\times\exp(\bar{\chi}^2\cos^2 2\theta)\}\ , \tag{16}$$

where

$$\mathrm{erf}(x)=\frac{2}{\sqrt{\pi}}\int_0^x e^{-t^2}dt \tag{17}$$

is the standard error function. $dP/d\theta$ is a decreasing function of θ. If statistical fluctuations are large compared to the dynamical anisotropy, that is, if $\bar{\chi}\ll 1$, Eq. (16) reduces to

$$\frac{dP}{d\theta}=\frac{2}{\pi}(1+\sqrt{\pi}\bar{\chi}\cos2\theta)+O(\bar{\chi}^2)\ . \tag{18}$$

The anisotropy results here in a small deviation, with an amplitude proportional to $\bar{\chi}$, from the constant value corresponding to isotropic emission. On the other hand, in the limit where $\bar{\chi}\gg 1$ (strong anisotropy), Eq. (16) becomes

$$\frac{dP}{d\theta}=\frac{4\bar{\chi}}{\sqrt{\pi}}\exp(-4\bar{\chi}^2\theta^2)\ . \tag{19}$$

In this case, the probability is a Gaussian of width $1/(2\sqrt{2}\bar{\chi})\ll 1$, centered at $\theta=0$. Note that Eq. (16) is of little practical use: θ is measured from the x axis which we have chosen, in this section, to be the direction of impact parameter x. But since there is no direct access to this direction in the experiment, θ, unlike α, is not an observable. We do not get any physical information from θ unless it is correlated with another independent evaluation of the reaction plane.

IV. REACTION PLANE CORRELATIONS

If one measures the reaction plane from $S^\perp$ in two separate rapidity intervals with the same multiplicity, one obtains two angles θ_1 and θ_2 (measured from an arbitrary fixed direction) which are two measurements of the reaction plane. The determination is reliable only if θ_1 and θ_2 are strongly correlated. In this section, we calculate the probability distribution $dP_{\mathrm{corr}}/d\theta$ of the relative angle $\theta\equiv\theta_1-\theta_2$. If this probability if flat, θ_1 and θ_2 are uncorrelated and no conclusion can be drawn concerning the occurrence of collective flow. We expect this to be the case if anisotropy is small or statistical fluctuations are large; that is, if $\bar{\chi}\ll 1$. If, on the other hand, $\bar{\chi}\gg 1$, we expect $dP_{\mathrm{corr}}/d\theta$ to be strongly peaked at $\theta=0$.

We shall assume that the rapidity intervals are well separated, so that there is no correlation between them, and consider the two corresponding sphericity tensors as statistically independent. Then θ_1 and θ_2 are two independent random variables. We further assume that macroscopic quantities (fluid velocity, energy density) are invariant under Lorentz boosts along the collision axis [10] and postpone the discussion of this point to Sec. VI. Since the sphericity tensor $S^\perp$ involves transverse coordinates only, it is also boost invariant. Thus $\bar{\alpha}$ and σ are the same for both rapidity intervals and θ_1 and θ_2 have the same probability distribution, given by Eq. (16). The correlation function is then given by

$$\frac{dP_{\mathrm{corr}}}{d\theta}=\frac{1}{2}\int_{-\pi/2}^{\pi/2}d\theta_1\int_{-\pi/2}^{\pi/2}d\theta_2\frac{dP}{d\theta}(\theta_1)\frac{dP}{d\theta}(\theta_2)\times\delta(\theta-\theta_1+\theta_2)$$
$$=\frac{1}{2}\int_{-\pi/2}^{\pi/2}d\theta_1\frac{dP}{d\theta}(\theta_1)\frac{dP}{d\theta}(\theta_1-\theta)\ , \tag{20}$$

where $dP/d\theta$ is given by Eq. (16). The factor $\frac{1}{2}$ normalizes $dP_{\mathrm{corr}}/d\theta$ to unity between 0 and $\pi/2$.

The integration can be carried out analytically (see Appendix A), which yields the results

$$\frac{dP_{\mathrm{corr}}}{d\theta}=e^{-\bar{\chi}^2}\left[\frac{2}{\pi}(1+\bar{\chi}^2)+\bar{\chi}^2[\cos2\theta(I_0+L_0)(\bar{\chi}^2\cos2\theta)+(I_1+L_1)(\bar{\chi}^2\cos2\theta)]\right]\ , \tag{21}$$

where I_0 and I_1 are modified Bessel functions of the first kind and L_0 and L_1 are modified Struve functions. Equation (21) reduces to

$$\frac{dP_{\mathrm{corr}}}{d\theta}=\frac{2}{\pi}+\bar{\chi}^2\cos2\theta \tag{22}$$

if $\bar{\chi}\ll 1$, and to

$$\frac{dP_{\mathrm{corr}}}{d\theta}=\left[\frac{8}{\pi}\right]^{1/2}\bar{\chi}\exp(-2\bar{\chi}^2\theta^2) \tag{23}$$

if $\bar{\chi}\gg 1$. These asymptotic forms can be deduced directly from Eqs. (18)–(20). Note that for small $\bar{\chi}$, the correlations (deviations from a flat probability) are of order $\bar{\chi}^2$. Thus, when statistical fluctuations become larger than dynamical effects, correlations decrease very quickly. On the other hand, if $\bar{\chi}\gg 1$, $dP_{\mathrm{corr}}/d\theta$ is the convolution of

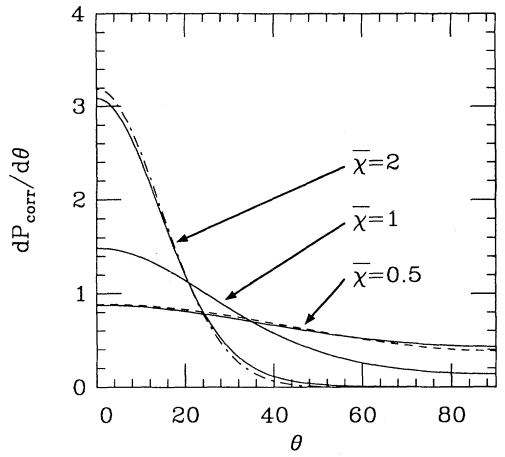

FIG. 2. Solid lines: correlation function defined by Eq. (21) for three values of $\bar{\chi}$. Dashed line: Small $\bar{\chi}$ approximation, Eq. (22). Dot-dashed line: large $\bar{\chi}$ approximation, Eq. (23).

two identical Gaussians (19), that is a Gaussian of width $1/(2\bar{\chi})$. The correlation function given by Eq. (21) is displayed in Fig. 2 for three values of $\bar{\chi}$, together with the approximations (22) and (23). One sees that these approximations are very good for $\bar{\chi} \leq 0.5$ and $\bar{\chi} \geq 2$, respectively.

A measure of the correlation strength is obtained by forming the ratio of the number of events with $\theta > 45°$ to the number of events with $\theta < 45°$. This ratio is equal to 1 if there is no correlation between reaction planes and vanishes if they are strongly correlated. Integrating Eq. (21) over θ, one obtains a simple analytic expression for this ratio (see Appendix A):

$$\frac{N_{\theta>45°}}{N_{\theta<45°}} = \frac{\int_{\pi/4}^{\pi/2} \frac{dP_{\rm corr}}{d\theta} d\theta}{\int_{0}^{\pi/4} \frac{dP_{\rm corr}}{d\theta} d\theta} = \frac{1}{2\exp(\bar{\chi}^2) - 1} . \quad (24)$$

This quantity is displayed in Fig. 3 as a function of $\bar{\chi}$. As expected, it decreases from 1 to 0 when $\bar{\chi}$ goes from 0 to $+\infty$. One observes that this ratio differs significantly from unity already for modest values of $\bar{\chi}$, so that collective effects should be seen easily by measuring reaction plane correlations. Any deviation of $dP_{\rm corr}/d\theta$ from a constant value can be attributed to collective flow (within our hypotheses), which makes this signature less ambiguous than that associated with the distribution of anisotropy (see Fig. 1 and the corresponding discussion in Sec. III).

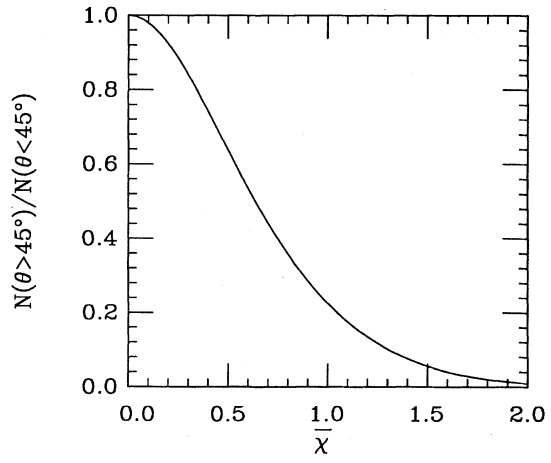

FIG. 3. Ratio defined in Eq. (24) as a function of the dimensionless parameter $\bar{\chi}$.

The ratio in Eq. (24) can be measured directly, and from its value one deduces the value of $\bar{\chi}$. One may then check whether Eq. (21) reproduces the observed behavior of the correlation function.

V. RELATION TO ANISOTROPY

The correlation between reaction planes clearly does not exhaust all the information we get from the sphericity tensor analysis. We also have a measurement of the anisotropy α. The value of $\bar{\chi}$ one gets from the analysis of plane correlations fixes the shape of the χ distribution, using Eq. (14). In order to get the α distribution, the scale factor σ is required [see Eq. (12)]. As we shall see shortly, this quantity can be determined through the measured average value of α, which we denote by $\langle \alpha \rangle$. It is directly proportional to σ.

When we studied reaction plane correlations in Sec. IV, only half of the detected particles (at most) could be used to construct the sphericity tensor since we needed two independent evaluations of the reaction plane in each event. On the other hand, when measuring the anisotropy distribution, it is better to use all the particles detected in the central rapidity region, in order to minimize statistical fluctuations. Then the value of $\bar{\chi}$ which has been determined from reaction plane correlation cannot be used directly in analyzing the α distribution. Since σ scales like $1/\sqrt{M}$ and $\bar{\alpha}$ is independent of M, $\bar{\chi}$ must be scaled like $\sqrt{M}$. If, for instance, the set of measured particles is divided into two approximately equal subsets for the measurement of reaction plane correlations, and then used as a whole for measuring the anisotropy distribution, the value of $\bar{\chi}$ must be multiplied by $\sqrt{2}$.

Let us now calculate the average value of α:

$$\langle \alpha \rangle = \sigma \langle \chi \rangle = \sigma \frac{\int \chi (dP/d\chi) d\chi}{\int (dP/d\chi) d\chi} . \quad (25)$$

The denominator of this expression is equal to unity since $dP/d\chi$ given by Eq. (14) is normalized to unity. To calculate the numerator, we integrate Eq. (14) by parts and use the relation

$$dI_1/dz = \frac{[I_0(z) + I_2(z)]}{2}$$

and Eq. (15) to calculate the remaining integrals. The result is

$$\langle \chi \rangle = \frac{\sqrt{\pi}}{2} \left[(1+\bar{\chi}^2) I_0 \left[\frac{\bar{\chi}^2}{2} \right] + \bar{\chi}^2 I_1 \left[\frac{\bar{\chi}^2}{2} \right] \right] \times \exp(-\bar{\chi}^2/2) . \quad (26)$$

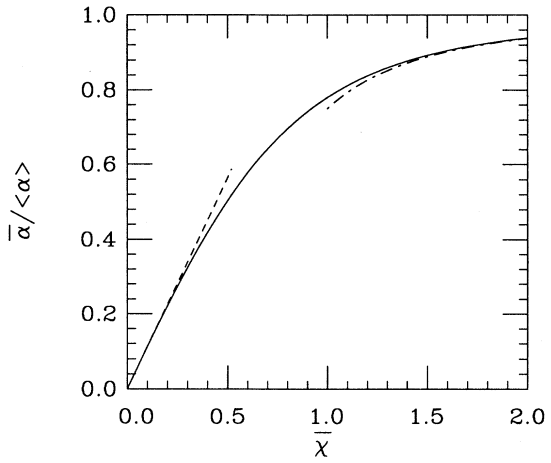

FIG. 4. Solid line: ratio of the "dynamical" anisotropy $\bar{\alpha}$ to the measured average value of α, denoted by $\langle\alpha\rangle$, as a function of $\bar{\chi}$. Dashed line: small $\bar{\chi}$ approximation, Eq. (28). Dot-dashed line: large $\bar{\chi}$ approximation, Eq. (29).

Thus, if one measures $\bar{\chi}$ and $\langle\alpha\rangle$, the last two equations give the scale factor σ and thus $\bar{\alpha}=\sigma\bar{\chi}$. From Eq. (25) one immediately gets

$$\bar{\alpha}/\langle\alpha\rangle=\bar{\chi}/\langle\chi\rangle \ . \tag{27}$$

This quantity is displayed in Fig. 4. For a small anisotropy, $\bar{\chi}\ll 1$, the χ distribution (14) is Gaussian and one gets

$$\bar{\alpha}/\langle\alpha\rangle\simeq(2/\sqrt{\pi})\bar{\chi} \ . \tag{28}$$

In this case most of the observed anisotropy results from fluctuations and the dynamical component $\bar{\alpha}$ is only a small fraction of the average anisotropy. On the other hand, for $\bar{\chi}\gg 1$, statistical fluctuations become negligible and the average anisotropy $\langle\alpha\rangle$ is close to $\bar{\alpha}$. Asymptotically,

$$\bar{\alpha}/\langle\alpha\rangle\simeq 1-1/(4\bar{\chi}^2) \ . \tag{29}$$

Once $\bar{\alpha}$ and σ are determined, the measured α distribution can be compared to the theoretical prediction, Eq. (14).

VI. DISCUSSION

Let us recall and discuss the hypotheses on which our calculations are based. The first hypothesis was made at the beginning of Sec. III, where we assumed that the sphericity tensor S_{ij} has a Gaussian distribution. This is true if it can be considered as the sum of a large number of independent sources, which is a reasonable assumption if the nucleon-nucleon collisions creating the particles are incoherent. However, deviations from this behavior can occur due to jets, which result in strongly correlated, strongly anisotropic emission of particles. At very high energies—for instance, at the CERN Large Hadron Collider (LHC)—one expects a large number of jets per event, and pairs of jets can be considered independent so that our statement holds: the only consequence is that the number of independent sources is the number of jets rather than the number of produced particles, so that we expect larger statistical fluctuations. On the other hand, if only a few jets (for example, one or two) are produced in each event, which may be the case at lower energies, significant deviations from the Gaussian distribution may occur. These would cause deviations of the anisotropy and angle distributions from the shapes predicted by our model, given by Eqs. (14) and (21).

The second hypothesis was made in Sec. IV where we treated the sphericity tensors measured in two separate rapidity intervals as independent variables. This is not strictly true if the rapidity intervals are too close to each other: for instance, a resonance decay or a pair of jets can give contributions to both rapidity intervals. This can be avoided by taking two remote rapidity intervals. This will be possible at the BNL Relativistic Heavy Ion Collider (RHIC) and LHC if detectors have a large rapidity acceptance. In current experiments at CERN and Brookhaven, the rapidity window is not so large and one may be constrained to work with adjacent rapidity intervals. One may check directly, as a test of statistical independence, that the value of $\bar{\chi}$ deduced from the analysis indeed scales like $\sqrt{M}$, with M being the number of particles used in the analysis.

We also assumed in Sec. IV that the probability distribution of $S^{\perp}$ was the same for both rapidity intervals as a consequence of Bjorken's scenario [10] for the fluid evolution. This scenario is known to be unrealistic in current experiments since the measured rapidity distributions are not flat. However, this hypothesis is not crucial here. It simplified the calculations since we used the same value of the scaled anisotropy $\bar{\chi}$ for both rapidity intervals. Without this hypothesis, we would not have obtained analytical expressions, but the qualitative ideas would remain the same. In particular, the correlation between reaction planes could still be used to identify collective flow. Note further that recourse to Bjorken's scenario can be avoided for a symmetric collision: if the two rapidity intervals are chosen symmetric of each other in the center-of-mass frame, they are equivalent by symmetry and the value of $\bar{\chi}$ is the same for both. Even more generally, it is reasonable to assume that the anisotropy $\bar{\alpha}$ depends only weakly on the rapidity since it is not much affected by the longitudinal expansion [5]. If the two rapidity intervals have the same multiplicity, the statistical fluctuations σ should also be comparable and therefore there is no reason for $\bar{\chi}$ to change drastically from one rapidity interval to another.

Although one must be careful in applying our results according to the above discussion, reaction plane correlations appear to provide a powerful tool for identifying collective flow. The ratio defined in Eq. (24) is very sensitive to collective effects: for $\bar{\chi}=0.3$, this ratio is about 0.85, and such a deviation from unity would be seen clearly in an experiment. We have shown [5] that the anisotropy distribution alone should allow one to identify collective flow at the BNL Alternate Gradient Synchrotron (AGS) and SPS with heavy nuclei (Au or Pb projec-

tiles). With the plane correlation method presented here, the possibility is not excluded that collective effects could be seen with lighter projectiles; for instance, with ^{32}S or ^{40}Ca beams on heavy targets.

Note added in proof. We would like to point out that some of our results can also be used in analyzing intermediate energy data with the method proposed by Danielewicz and Odyniec [3]. These authors measure the reaction plane by constructing the transverse momentum transfer **Q** between target and projectile. **Q** is an *oriented* vector in the transverse plane, whose azimuthal angle φ may vary between 0 and 2π. In contrast, the eigenaxis of our sphericity tensor S_{ij} is not oriented, and its azimuthal angle (which we denote by θ) varies between 0 and π only. However, **Q**, as S_{ij}, is the sum of a large number of independent contributions and, therefore, has a Gaussian distribution. Its distribution is given by Eq. (10), in which one replaces α and $\bar{\alpha}$ by Q and $\bar{Q} \equiv |\langle \mathbf{Q} \rangle|$ and 2θ by φ. The width σ in Eq. (10) becomes then a measure of fluctuations of **Q** due to finite multiplicity. Introducing the variable $\chi = Q/\sigma$, the χ and ϕ distribution are then given by Eqs. (14) and (16), and the average value of $\cos\varphi$ is

$$\langle \cos\varphi \rangle = \frac{\sqrt{\pi}}{2} \bar{\chi} e^{-\bar{\chi}^2/2} (I_0 + I_1)(\bar{\chi}^2/2) \ .$$

In order to estimate the accuracy of their transverse momentum analysis, Danielewicz and Odyniec divide each event randomly into two subevents, measure **Q** in each subevent, and study the azimuthal angle distribution $dN/d\varphi$ of the two vectors with respect to each other. This is similar to the method proposed in Sec. IV of this paper, and $dN/d\varphi$ is equal to our $dP_{\rm corr}/d\theta$ in Eq. (21). We have checked numerically that the various Monte Carlo results presented in Ref. [3] are perfectly reproduced by our analytical formulas in which one takes $\bar{\chi} \simeq 0.87$ for the whole set of measured particles. This gives a measure of the ratio of collective effects to statistical fluctuations in intermediate energy nuclear collisions.

ACKNOWLEDGMENTS

I thank H. Gutbrod for stimulating discussions and J.-P. Blaizot for carefully reading the manuscript.

APPENDIX A: DERIVATION OF THE CORRELATION FUNCTION

Inserting Eq. (13) in Eq. (20) one may write the correlation function in the form

$$\frac{dP_{\rm corr}}{d\theta} = \frac{8}{\pi^2} \exp(-2\bar{\chi}^2) \int_0^{+\infty} \chi_1 d\chi_1 \int_0^{+\infty} \chi_2 d\chi_2 \exp(-\chi_1^2 - \chi_2^2) \times \int_{-\pi/2}^{\pi/2} d\theta_1 \exp[2\bar{\chi}\chi_1 \cos 2\theta_1 + 2\bar{\chi}\chi_2 \cos 2(\theta_1 - \theta)] \ . \tag{A1}$$

This can be integrated over θ_1 by using the modified Bessel function I_0:

$$\int_{-\pi/2}^{\pi/2} d\theta_1 \exp(A \cos 2\theta_1 + B \sin 2\theta_1) = \pi I_0(\sqrt{A^2 + B^2}) \ . \tag{A2}$$

This gives

$$\frac{dP_{\rm corr}}{d\theta} = \frac{8}{\pi} \exp(-2\bar{\chi}^2) \int_0^{+\infty} \chi_1 d\chi_1 \int_0^{+\infty} \chi_2 d\chi_2 \exp(-\chi_1^2 - \chi_2^2) I_0(2\bar{\chi}\sqrt{\chi_1^2 + \chi_2^2 + 2\chi_1\chi_2 \cos 2\theta}) \ . \tag{A3}$$

Introducing polar coordinates in the (χ_1, χ_2) plane, defined by $\chi_1 = r\cos\phi$, $\chi_2 = r\sin\phi$, with $r \geq 0$ and $0 \leq \phi \leq \pi/2$, the integral over r is of the type

$$\int_0^{+\infty} dr\, r^3 \exp(-r^2) I_0(ar) = \frac{1}{2} \left[1 + \frac{a^2}{4} \right] \exp\left[\frac{a^2}{4} \right] \tag{A4}$$

as may be checked by expanding I_0. Equation (A3) thus becomes

$$\frac{dP_{\rm corr}}{d\theta} = \frac{2}{\pi} e^{-\bar{\chi}^2} \int_0^{\pi/2} d\phi \sin 2\phi [1 + \bar{\chi}^2 (1 + \sin 2\phi \cos 2\theta)] \exp(\bar{\chi}^2 \sin 2\phi \cos 2\theta) \ . \tag{A5}$$

Note that the integrand is invariant under $\phi \to \pi/2 - \phi$, which reflects the fact that χ_1 and χ_2 play symmetric roles in Eq. (A1). The integration range can then be restricted to the interval $[0, \pi/4]$. Making the change of variables $\pi/2 - 2\phi \to \phi$, the integral can be expressed in terms of the modified Bessel functions

$$I_0(z) = \frac{2}{\pi} \int_0^{\pi/2} \cosh(z \cos\phi) d\phi \ ,$$
$$I_1(z) = \frac{2z}{\pi} \int_0^{\pi/2} \sin^2\phi \cosh(z \cos\phi) d\phi \tag{A6}$$

and the modified Struve functions [11] $\mathbf{L}_0(z)$ and $\mathbf{L}_1(z)$ which have expressions similar to I_0 and I_1, with cosh replaced by sinh. After integration by parts, Eq. (A5) yields the result

$$\frac{dP_{\rm corr}}{d\theta}=e^{-\bar{\chi}^2}\left[\frac{2}{\pi}(1+\bar{\chi}^2)+\bar{\chi}^2[\cos2\theta(I_0+\mathbf{L}_0)(\bar{\chi}^2\cos2\theta)(I_1+\mathbf{L}_1)(\bar{\chi}^2\cos2\theta)]\right] \tag{A7}$$

identical to Eq. (21). Let us check that this expression is normalized to unity when integrated from 0 to $\pi/2$. The functions $\cos2\theta I_0(\bar{\chi}^2\cos2\theta)$ and $I_1(\bar{\chi}^2\cos2\theta)$ are odd in $\cos2\theta$ and thus do not contribute to the integral. Using the relations $I_1(z)=dI_0/dz$ and $\mathbf{L}_1(z)=d\mathbf{L}_0/dz+2/\pi$ and the definitions (A6), the integrals of Struve functions can be expressed in terms of integrals of Bessel functions, which can be found in the literature or calculated directly by a power-series expansion:

$$\int_0^{\pi/2}d\theta\,\mathbf{L}_1(\bar{\chi}^2\cos\theta)=-1+\int_0^{\pi/2}d\phi\,\cos\phi I_0(\bar{\chi}^2\cos\phi)$$
$$=-1+\frac{\sinh\bar{\chi}^2}{\bar{\chi}^2} \tag{A8}$$

and

$$\int_0^{\pi/2}d\theta\,\cos\theta\mathbf{L}_0(\bar{\chi}^2\cos\theta)=\int_0^{\pi/2}d\phi\,I_1(\bar{\chi}^2\cos\phi)$$
$$=\frac{\cosh\bar{\chi}^2-1}{\bar{\chi}^2}\ . \tag{A9}$$

Normalization of the probability (A7) follows immediately.

Let us finally calculate the ratio defined in Eq. (24). Since the correlation function (A7) is normalized to unity, we only need to calculate $\int_{\pi/4}^{\pi/2}(dP_{\rm corr}/d\theta)d\theta$. On this interval, all the terms in Eq. (A7) give a nonvanishing contribution. However, using Eqs. (A8) and (A9) one obtains

$$\int_{\pi/4}^{\pi/2}d\theta\,\cos2\theta I_0(\bar{\chi}^2\cos2\theta)$$
$$=-\frac{1}{2}-\int_{\pi/4}^{\pi/2}d\theta\,\mathbf{L}_1(\bar{\chi}^2\cos2\theta) \tag{A10}$$

and

$$\int_{\pi/4}^{\pi/2}d\theta\,I_1(\bar{\chi}^2\cos2\theta)=-\int_{\pi/4}^{\pi/2}d\theta\,\cos2\theta\mathbf{L}_0(\bar{\chi}^2\cos2\theta)\ . \tag{A11}$$

The terms involving Bessel functions and Struve functions in Eq. (21) thus cancel pairwise in the integration and one gets

$$\int_{\pi/4}^{\pi/2}\frac{dP_{\rm corr}}{d\theta}\,d\theta=\frac{1}{2}\exp(-\bar{\chi}^2)\ , \tag{A12}$$

from which Eq. (24) immediately follows.

[1] H. Gustafsson *et al.*, Phys. Rev. Lett. **52**, 1590 (1984).

[2] WA80 Collaboration, H. R. Schmidt *et al.*, in *Quark Matter '87,* Proceedings of the Sixth International Conference on Ultrarelativistic Nucleus-Nucleus Collisions, Munster, West Germany, 1987 [Z. Phys. C **38**, 109 (1988)].

[3] P. Danielewicz and G. Odyniec, Phys. Lett. **157B**, 146 (1985).

[4] N. S. Amelin *et al.*, Phys. Rev. Lett. **67**, 1523 (1991).

[5] J.-Y. Ollitrault, Phys. Rev. D **46**, 229 (1992).

[6] H. H. Gutbrod *et al.*, Phys. Lett. B **216**, 267 (1989); H. H. Gutbrod *et al.*, Phys. Rev. C **42**, 640 (1990).

[7] J.-Y. Ollitrault, in *Proceedings of the Second International Conference on Physics and Astrophysics of Quark-Gluon Plasma,* Calcutta, India, 1993 (World Scientific, Singapore, in press).

[8] This was discussed in the context of intermediate energies by P. Danielewicz and M. Gyulassy, Phys. Lett. **129B**, 283 (1983).

[9] M. Gyulassy *et al.*, Phys. Lett. **110B**, 185 (1982).

[10] J. D. Bjorken, Phys. Rev. D **27**, 140 (1983).

[11] H. Bateman, *Higher Transcendental Functions,* (McGraw-Hill, New York, 1953), Vol. 2.